Invited Paper

SELF-ORGANIZATION IN NON-CRYSTALLINE SOLIDS

M. Popescu[*]

National Institute of Materials Physics, 76900-Bucharest-Magurele,
P. O. Box MG. 7, Romania

It is shown that self-organization can be revealed in non-crystalline materials. Experimental and modelling studies are discussed. The importance of the Boolchand intermediary phase for the chalcogenide network glasses with self-organization is pointed out. The basical principles of self-organization are the key for the production of nano-materials with new properties.

1. Introduction

Amorphous, glassy, and, in general, disordered materials are governed by laws not completely understood up to day. The metastable configuration of the atoms gives to material the possibility to choose one among various pathways to change its free energy when, by providing some energy, the system is pushed to modify the quasi-equilibrium states in one of the multiple states of higher/lower energy. Small steps that ensure the adiabatic phase-change accomplish this task. During energy action a self-organized state can be reached. The self-organization phenomenon ensures the reversibility of the atomic state during energy exchange with the surrounding medium.

The self-organization leads to a new structure for the non-crystalline materials, the so-called nanostructure. More and more arguments support the nanostructured configuration of the amorphous films or glassy materials and the basical ideas and concepts used for the understanding of their electronic properties are developing [1].

In this paper we try to demonstrate by simulation procedures applied to structural models, the nanostructural arrangement in basical non-crystalline solids used in electronics and optoelectronics: amorphous silicon and chalcogen-based materials.

2. Amorphous silicon

2.1. Modelling of the nano-structure

One of the materials developed in applications was amorphous hydrogenated (halogenated) silicon. The question [2] whether a structural state exists in hydrogenated amorphous silicon (a-Si:H) between the amorphous state of short-range order and the microcrystalline state of long-range order has stimulated a renewed interest. This state of intermediate order might be disordered enough to spoil the crystalline selection rules for optical transitions, hence providing for the strong optical absorption desired in photovoltaic devices (e.g. solar cells). It may be yet ordered enough to inhibit any structural changes and photoinduced defects that decrease the photocarrier lifetimes. Such a decrease ultimately leads to reduced efficiencies of these photovoltaic devices during long light exposure. The decrease or elimination of this degradation, which is called the Staebler-Wronsky degradation (SWD) after its discoverers [3] is one of the major goals in the research of a-Si:H and related materials.

The understanding of device stability is increasingly focused on the nature of heterogeneity within the amorphous silicon material [4]. Detailed studies have been carried out and rewarding

---

[*] Corresponding author: mpopescu@alpha1.infim.ro

results were obtained. An intermediately ordered phase of silicon has been suggested to be implicated in both amorphous and microcrystalline a:Si:H [5]. Tsu et al. [6] have shown that in a-Si:H special chain-like objects (CLO) at the nanometer scale are produced. These CLO's are quasi-one-dimensional, having 2-3 nm widths and lengths of ~30 nm or more. Significantly, they show a high degree of order along their length, implying very low levels of bond angle distortion. It is remarkable that the high quality a-Si:H material used in the production of solar cells having superior photoelectronic performance, especially in regard to the Staebler-Wronski degradation effect, has elevated levels of CLO's. This enhanced performance seems to be a result of the intermediate order of the CLO's, that are essentially strain-free. With this sort of heterogeneity, an a-Si:H film can reach an overall more relaxed state than it could if it were composed of a homogeneous amorphous matrix. This sort of heterogeneity, comprised of the CRN and the quasi-linear CLO components, should offer few interfacial defects, compared to (say) the CRN and the rather rigid three-dimensional microcrystalline structure.

The disordered, amorphous state of silicon, and germanium was firstly thought in terms of the continuous random network (CRN) models for the atomic arrangement. The first CRN model was developed by Polk [7] for amorphous germanium. Later, Steinhardt et al. [8] and Popescu [9] succeeded to find more realistic models by using a Monte Carlo procedure for free energy minimization in the models. The Keating approximation for the covalent bond [10] and the force constants deduced by Martin [11] were used in the calculations. An excellent agreement of the structural data (radial distribution function, density) deduced from the CRN model with those experimentally found for germanium proved the general validity of the model. Moreover, the calculated free energy of the CRN model is in fairly good agreement with the crystallization energy of germanium as known from the literature [12].

In order to investigate the structure of amorphous silicon and to see how the energetical factors influence the structural details, we developed several random network models with various numbers of atoms.

The models were relaxed with the stretching bond force constant α and bending bond force constant β in the frame of the Keating approximation for the covalent bond [10] with the values given by Martin [11]. In Table 1 are put together the structural and energetical data for the first relaxed CRN model of silicon with 155 atoms, for the biggest relaxed model of a-Si with 2052 simulated atoms, and for the CRN model with only even-fold rings/mostly 6 and 8-fold rings/ (156 atoms). The modelling data are compared with the experimental data on amorphous silicon. There are shown the rms deviations of the first and second order distance due only to structure, as calculated in [13].

Table 1. Structural and energetical data for CRN models of amorphous silicon.

a-Si models	CRN(155)	CRN(2052)	CRN(156)	a-Si (experim.)[13]
5-fold/6-fold rings	0.60	0.48	0	-
7-fold/6-fold rings	0.84	1.09	0	-
rms deviation of bonding distance (Å)	0.036	0.067	0.095	0.089
rms deviation of second order distance (Å)	0.198	0.259	0.304	0.249
rms tetrahedral angle distortion	6.684 $^\circ$	9.977°	13.601 $^\circ$	9.6 $^\circ$ 10 $^\circ$ [6]
mean bond stretching energy per bond ($\times 10^{-5}$ dyn.Å)	0.1653	0.5854	0.8513	-
Mean bond bending energy per bond ($\times 10^{-5}$ dyn.Å)	0.3394	0.7617	1.4238	-
total free energy per bond ($\times 10^{-5}$ dyn.Å)	0.5047	1.3471	2.2751	-

The highest free energy is characteristic to the model with even-fold rings of atoms: CRN(156). The largest CRN model (with 2052 atoms and a diameter of ~4 nm) shows the largest free energy, if compared to the other CRN models with a mixture of even and odd rings of atoms. The BAD becomes larger when the percent of five-fold rings decreases.

The calculation has shown that dihedral angles are not uniformly distributed. The CRN(155) and CRN(156) models favor a more uniform dihedral angle distribution while the CRN(2052) model shows a dihedral distribution with a significant but large maximum around the dihedral angles of 60° and 180° this values accounting for a preferred staggered configuration of the atoms. This aspect seems to be not related to the percent of the 5-fold rings in the models with odd and even rings of atoms.

CRNs are ideal networks and can be rarely produced. In fact they must include an enough large amount of free energy due to growing misfit in the compact arrangement of atoms when the volume of CRN increases. This misfit appears e.g. when the crystalline like arrangement of the tetrahedral units in germanium and silicon is substituted by dodecahedral-pentagonal configurations (amorphons or modified Voronoi polyhedra) [14], which are incompatible with the long-range order characteristic to crystal. With this idea in mind we tried [15] to see what happens if a model of amorphous silicon, of minimum free energy is split in two amorphous domains, which, subsequently, were relaxed separately. A model of amorphous silicon with 405 atoms (diameter ~2.5 nm) with two domains (amorphites) was developed. Table 2 shows the free energy data after computer relaxation of the model as a whole (M) and for the two separated and relaxed domains (M1 and M2).

Table 2. The free energy and structural characteristics of the CRN(405) relaxed model of
amorphous silicon before and after separation in two domains.

Models	Bond stretching energy $\times 10^{-2}$ dyn.Å	Bond bending energy $\times 10^{-2}$ dyn.Å	Total free energy $\times 10^{-2}$ dyn.Å	Bond angle distortion (^{o})	rms bond distortion (Å)	rms 2-nd order distance (Å)
M (405 atoms)	0.5378	1.620	2.157	10.200	0.072	0.266
M1 (200 atoms)	0.1256	0.5593	0.6849	9.100	0.053	0.246
M2 (205 atoms)	0.1299	0.5253	0.6552	8.841	0.053	0.245
M1 + M2	0.2555	1.0846	1.3401	8.971	0.053	0.2455

As can be seen from the Table 2 the splitting of the CRN (405) model for amorphous silicon allows for a significant diminishing of the total free energy of the model.

These results has lead us to the idea that a true, realistic model of tetrahedrally bonded amorphous semiconductors must suppose a meander-like structure, where CRN domains of limited size create an entanglement of fine inter-domains boundaries which are extended over all the volume of the material. This new picture for amorphous semiconductors can open the way toward understanding the specific phenomena observed experimentally as e.g. centers of defects different from dangling bonds, hydrogen diffusion, aging, etc. In fact, symmetry breaking in continuous random networks seems to be a natural concept, usually encountered in many phenomena from the nuclear physics to astrophysics.

If the symmetry is broken and several domains are formed, is it possible to get a state of lower free energy, as a consequence of self-organization? The separation of the models in several domains gives rise to boundaries, which must be compared, to the experimentally observed CLO's [6].

During nanostructuration with the formation of inter-domain boundaries hydrogen diffuses at the surface of the amorphous domains. The surface is stabilized with low distortion bonds and crystalline-like organization. The formation of a fractal surface that minimizes the free energy of the surface is probably the characteristic feature in this case.

The energy introduced in the nanostructured system can shift the equilibrium of the atom network. The amorphous domains can be 're-amorphized' and a new melted/solidified phase with different characteristics can be reached. High-energy irradiation rises the metastability minimum of

the amorphous phase, while low energy irradiation can trigger modifications according to which the system descends to a lower metastability minimum. Thus, a fine-tuning by switching to various configurations in a reversible manner can be obtained.

The simulations performed for a-Si point out the natural tendency of the a-Si material to divide in small domains separated by boundaries, i.e. to become nanostructured. The boundary atoms take a structural configuration with low distortion bonds, and crystalline-like (diamond and/or wurtzite) arrangement. A tentative simulation of crystalline-like arrangement at the boundary between two CRN domains was carried out on a CRN model with 499 atoms, Mixt499.

We introduced two silicon layers (2×47 atoms), one layer connected to the amorphite M1 and the other to the amorphite M2 of the CRN (405) model (44 links). Thereafter, the two amorphites were merged by the intermediary of the dangling bonds at the surface of every extended amorphite. A new CRN model with 499 atoms has been thus obtained. This model was relaxed. In the second stage we changed topologically the two layers in order to obtain a crystalline-like configuration (6-fold, chair-like rings), thus simulating the crystallization of a thin region situated in-between the amorphites. A new relaxation was performed. In the next stages the crystallized region with a thickness of ~0.5 nm and the diameter of ~2.5 nm was decoupled step by step from the bodies of the amorphites by cutting a percent of the links with amorphites, starting with the most distorted bonds (models: Decoupl. 1-5, Table 3). After relaxation, the structural and energetical parameters were calculated for every step of simulation both for the diamond-like crystalline configuration and for the rest of the amorphites. The results are shown in Table 3.

Table 3. The structural and energetical parameters for the CRN(499) model for amorphous
silicon with crystallization at the interface of the amorphous domains.

Model	Decoupl. Bonds (%)	rms(r_1) (Å)	rms(r_2) (Å)	BAD (^{o}) Crystall.|Amorphite|		Stretching energy $\times 10^{-2}$dyn.Å	Bonding energy $\times 10^{-2}$dyn.Å	Total energy $\times 10^{-2}$dyn.Å
Mixt 499	0	0.070	0.265	10.735	9.748	0.5587	1.8400	2.3986
Cryst 499	0	0.068	0.256	6.020	9.715	0.5378	1.6197	2.1575
Decoupl 1	21	0.065	0.255	5.144	9.523	0.4628	1.4578	1.9207
Decoupl 2	38	0.065	0.252	4.457	9.397	0.4281	1.3631	1.7910
Decoupl 3	54	0.062	0.249	4.043	9.340	0.4071	1.3105	1.7176
Decoupl 4	69	0.060	0.246	3.261	9.233	0.3593	1.2371	1.5963
Decoupl 5	75	0.055	0.246	2.629	9.111	0.3080	1.1780	1.4860

It is remarkable that bond angle distortion (BAD) in the crystallized layer diminishes step by step when the coupling with the amorphites becomes poorer. This means that the thin crystallite becomes more free of constraints and takes a more and more correct structure. Finally for 75 % reduction of the bonding constraints with the amorphites, the BAD reaches the value of 2.629^o. This corresponds to 11 bonds between crystallite and amorphites from a total of 44 bonds acting in the initial topological configuration. The low value of the BAD is to be compared with the experimental value deduced for CLO's observed in TEM and characterized by Raman scattering: BAD ~ 0°. The agreement is fairly good. As resulted from our simulation experiments the main aspect of the formation of a crystallite with low distortion of the bonds is the decoupling of the most part of its bonds with the amorphous network. This is undoubtedly triggered by the presence of the hydrogen, which diffuses and satisfies the dangling bonds appeared during formation of the crystalline thin film. Only in amorphous hydrogenated silicon with enough high concentration of hydrogen it is possible to have such diffusion process with the satisfaction of the dangling bonds and separation of the crystalline configurations in-between the amorphous domains of the material.

Amorphous hydrogenated silicon of improved quality for photovoltaic devices can be prepared by hydrogen dilution of the processing gas. This increase in quality, as measured, for example, by a decrease of the Staebler-Wronski degradation, is accompanied by an increase in the concentration of chain-like objects, CLO's in TEM micrographs. The formation and the particular features of CLO's can be explained on the basis of nanostructuration in CRN networks of amorphous

silicon by splitting the rather uniform structure in homogeneous and less constrained domains linked through low distortion crystallite-like configurations. It seems that hydrogen (H) or fluorine (F) are playing in amorphous silicon the role of glass modifiers as Na or Ca atoms are playing in a-SiO$_2$ when silicate glasses are formed, i.e. conferring to structurally deficient, but interconnected network, a polymeric character.

As opposite to microcrystalline and nanocrystalline silicon, which are composed from crystalline domains surrounded by amorphous boundary layers, the device quality silicon can be viewed as composed from amorphous nano-domains surrounded by crystalline boundaries. The crystalline arrangement can be diamond-like or a mixture of diamond-like and wurtzite-like configurations due to constraints at boundaries, which allow for eclipsed orientation of the bonds. The high quality amorphous silicon is in fact a new-type of self-organized structure characterized by meander-like crystalline configurations that defines the rather homogeneous amorphous domains. This type of silicon will be called nano-amorphous silicon because it is a reverse structure of nano-crystalline silicon, a well-known material.

The importance of d–orbital bonding both in amorphous tetrahedrally semiconductors and in chalcogenide glasses is remarkable.

In amorphous silicon (germanium models) the contribution of d-orbital bonds has an essential effect in relieving the stresses in the region between the amorphous domains. Thus, the boundaries become thin low-dimensional unstressed and undistorted regions protruding deeper into the material, as observed in TEM pictures. It was shown earlier [16] that the distortion of the local tetrahedral symmetry of atomic bonds in a semiconductor like silicon always leads to such a change in the bond character as to eliminate elastic stresses. This can be achieved for metastable silicon phases by adding small d contribution to the usual sp^3 orbitals. On the basis of a tight binding calculation of the valence band density of states we have demonstrated that the atomic spd orbitals ensuing from this approach yield the correct valence band density of states in CRN(155) and CRN(2052) models.

The stability of the nanostructured amorphous material depends on the way of impeding grain boundary motion. The driving force for such motion is simply the reduction of the total area of grain boundary. This is because the boundaries exhibit a larger free energy, as shown in the CRN models. If the specific energy of the boundary can be made zero or negative, then the driving force for the grain growth vanishes. The domain structure is stable. John Weissmüller [17] advanced this idea in a quantitative form. The basically mechanism is, in its view, the segregation of a minor constituent solute. If, in our case, the hydrogen is the minor constituent solute in amorphous silicon, when the CRN grain grows, less segregated hydrogen is needed because the area of the boundary per unit volume decreases and, thus, the excess hydrogen returns in the grain. The returning of hydrogen in the amorphite enhances the free energy of the amorphite, so that the total free energy change is positive. If this occurs, then the driving force for the amorphite growth vanishes. We are dealing with a grain structure stabilized by segregation. If the hydrogen dilution rate in silane increases, at the temperature of 300 $^\circ$C takes place a motion of the boundary by hydrogen diffusion in the inner part of the amorphite. Consequently, the inter-domain region becomes labile and suffers an ordering process, by forming CLO's configurations, i.e. two-dimensional crystalline zones. These crystalline-like configurations stabilize the structure with small-size amorphous domains, well ordered as ideal amorphous phase. The molecular hydrogen seems to be the most important constituent solute for the migration in the amorphites, because other fragments obtained during silane decomposition are heavier and their diffusion is greatly impeded. As concerning the diffusion process, we must observe that high electronegative hydrogen or/and fluorine are able to break up the rather perfect covalent network of silicon. Halogens can be regarded as network modifiers. The adding of an electropositive modifier depolymerizes the structure of amorphous silicon (just as in the case of silicate glasses), with more destructive effect, more concentration of hydrogen is added. The depolymerization of the silicon network seems to be just the factor, which control the separation of the crystalline configurations at the boundaries.

2.2. The void structure of silicon and its relevance for the medium range order of the amorphous structure

Last years, an increased attention was paid to the problem of interstitial voids in the disordered materials with the purpose to explain some properties of the glasses. Thus, Elliott [18]

explained the structural origin of the first sharp diffraction peak in the diffracted intensity curves of several glasses through the void-based model, while Jensen et al. [19] suggested that voids are important for the interpretation of the positron annihilation lifetime data in non-crystalline chalcogenides.

The presence and the role played by the structural voids in various metal-semiconductor alloys as e.g. Ge-Mo and Ge-Au, are still under debate and several models based on the Monte Carlo – Metropolis and reverse Monte-Carlo methods have been discussed [20,21]. Recently, Gaskell [22] has reviewed the structural network glasses and has shown that ordered (microcrystalline) and random models have both strengths and weaknesses. Halm et al. [23] have shown that in many liquid alloys there are strong fluctuations of density at the atomic scale and they can be ascribed to the specific distribution of the voids.

An interstitial void in a lattice or network is defined as that region situated in-between the atoms, that corresponds to the sphere of maximum diameter, which can be introduced in the free space delimited by the atomic neighborhood [24]. The void size distribution represents the distribution of the diameters of all the spheres that can be introduced in the lattice or network without a notable superposition (partial superposition of around one tenth of the diameter was permitted, thus accounting for eventually non-spherical, elongated voids [25]). A special computer program run in FORTRAN was devised to this purpose.

We have calculated the distribution of the void size (diameters) in a continuous random network model of silicon with 2052 atoms: CRN (2052). The structure factor for the model, represented in Fig. 1a, agrees excellently with the experimental structural factor (see [26]). We have calculated the structure factor for a hypothetical network formed by the system of voids in this model. The curve is represented in Fig. 1b. Two observations must be made. Firstly, the voids lack short-range order and this fact is revealed by the absence of the oscillations in the structure factor for high values of the scattering vectors. Secondly, the voids lack long-range order and this is revealed by the absence of narrow peaks in the structure factor. Nevertheless, several significant but vanishing peaks situated at low Q prove the existence of some kind of order in the model. It is logically to admit that this is the medium-range order. Which are the characteristics of this ordering that be reflected also in the ordering of atoms? To have an answer we have tried to annihilate the effect of the voids in the model by introducing hypothetical atoms in the centres of the voids. The structure factor calculated after all the voids were "killed" is shown in Fig. 1c. It is clearly seen that the effect of void killing is the disappearance of the first peak in the structure factor of amorphous silicon situated at $Q = 20$ nm^{-1}. We can conclude that the disposal of the atoms on the inner cages defined by the random tetrahedrally network contains a minimum order (related to the positions of the third up to the sixth-order atomic neighbors) that can be regarded as the embryo of MRO. Therefore, the self-organization in amorphous tetrahedrally bonded networks is related to the atomic ordering on the boundary of the interstitial voids. This is an intrinsic property of such networks.
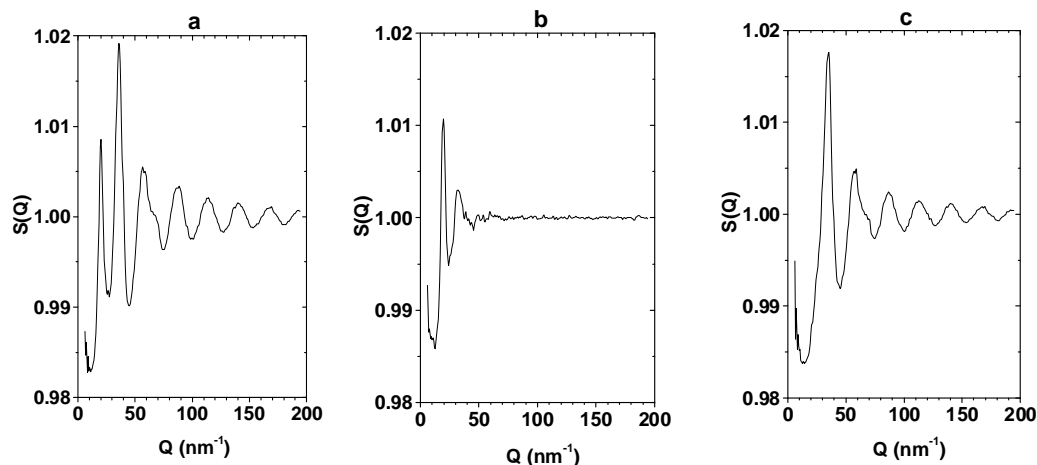

Fig. 1. The structure factor of the CRN model with 2052 atoms for amorphous silicon; a. structure factor for the network of 2052 atoms; b. structure factor for the void system; c. structure factor for the model with void centres occupied by atoms.

3. The self-organization in chalcogenide glasses

3.1. The Boolchand phase and its relevance for self-organization

The notion of global connectivity has played a useful role to understand the physical behaviour of network glasses and amorphous thin films. The idea emerged in embryonic form in the early seventies as material properties [27] of the chalcogenides were examined as a function of composition. However, it was not until the early eighties that a theoretical foundation evolved with the recognition that bonding interactions in covalent glasses form a hierarchy, and that nearest-neighbour valence interactions can serve as lagrangian constraints [28]. This led to the prediction of floppy to rigid phase-transition in network glasses, when the number of constraints per atom increases to 3. A mean co-ordination number of 2.40 in the network was discovered to be the rigidity transition by J. C. Phillips and M. F. Thorpe [28,29]. Recently P. Boolchand [30] revealed not one transition, but two rigidity transitions in the network glasses. The two transitions define the limits of an intermediate phase that separates the floppy from the stressed rigid phase. This intermediate phase is called *Boolchand phase* and is of high relevance in many other fields as e.g. protein folding, phase diagrams and high Tc superconductors.

New insights into the nature of glass transitions, and self-organization of molecular networks have emerged from T-modulated Differential Scanning Calorimetry (MDSC) [30-34]. The method permits separating the endothermic heat flow near T_g into two parts: an ergodic fraction (thermally reversing heat flow) and a non-ergodic one (non-reversing heat flow). The MDSC shows the non-reversing heat flow near T_g to display a sharply defined global minimum (in the case of Ge_xSe_{1-x} : $0.20<x<0.23$ and in the case of P_xSe_{1-x} glasses $0.28 <x<0.40$) identified with the self organized or Boolchand phase. It was shown that two distinct morphologies exist: chalcogen rich and pnictide (or germanium) rich phase separated at the nanoscale. Georgiev et al. [35] have shown that As_2Se_3 and $GeSe_2$ consists of a Se-rich majority phase that is separated from a compensating Ge- or As- rich minority phase. These phases do not mix, and are reflected in the thermally reversing character of the T_g's and the sharpness of the thermally reversing window. Wang et al. [36]. have shown that the network in the Boolchand phase is rigid but is formed with less (or not) overstressed region with the help of self-organization. With the help of self-organization processing, some constraints are removed from the overstressed region to apply on some floppy units. This process decreases the global constraints on the overconstrained region through sacrificing the degrees of freedom of the floppy region locally.

The threshold behaviour observed in binary Ge_ySe_{1-y} and As_xSe_{1-x} glasses [37] , near $y=1/3$ and $x = 2/5$, respectively, is considered as an evidence for nanoscale phase separation of these stoichiometric glasses.

All the experimental data speak in favour of the self-organisation of the glasses with special features depending on composition.

We must remark that other authors, as e.g. Minaev [38,39], tried to demonstrate that nano-heteromorphism and co-polymerization are necessary and sufficient conditions for glass-formation of mono- and multi-component glasses.

The recent results of the simulation of the complex polymerization-destruction processes show that in the amorphous chalcogenides a structural state based on fractal clusters occurs [40]. The model with competitive creation-destruction-switching processes seems to be able to explain various effects produced in non-crystalline chalcogenides under the influence of light irradiation. The self-assembly of the basical structural units with specific properties is an important feature of the model.

The principles of self-organization (phase separation, fractal growth...) seem to be essential in the explanation of the anisotropic phenomena induced by light only in non-crystalline chalcogenides and not in crystalline ones. Lyubin and Klebanov [41] claimed that in each of the excitation range (above-band-gap, sub-band-gap and super-band-gap excitation) different mechanisms are responsible for the appearance of the photoinduced anisotropy, Oriented creation of bunches of defects, orientation of some structural units, growth of ordered domains and even oriented nano-crystallization are considered [42].

3.2. The void structure of As-Ch glasses and the medium range order

The structure of the binary chalcogenide glasses has been analysed, based on the model of a typical network for As_2S_3 glass. The model comprises 802 atoms, was built by hand from the elemental plastic units and was relaxed by computer. Fig. 2a shows the structure factor of the model. The first sharp diffraction peak is clearly shown at Q ~ 15 nm^{-1}. We have calculated the void size distribution in the model by using the same procedure as in the case of amorphous silicon model. Again we calculated the structure factor of the void system (Fig. 2b). Two important peaks speak in favour of the remarkable medium range ordering of the voids. Finally we "killed" the voids by introducing hypothetical atoms in the centres of the voids. The new structure factor obtained in the hybrid model is represented in Fig. 2c. What is remarkable is nearly the disappearance of the first sharp diffraction peak. This is a proof in favour of the relation between the FSDP and the void structure. In the same time we have a proof for the fact that the atoms that define the voids are subjected to some kind of ordering.

Although not large separation of nano-phases were permitted in the model, the results show that further improvement of the model, in order to reproduce the fine details in the experimental structure factor, must be related to the spatial extension of the As-based layers, that improves the intensity of the FSDP, as evidenced experimentally. It is expected that Boolchand-type phase of the chalcogenide glasses be the best model for these glasses. The model with nanoscale phase separation by changing the interconnections in the old model is now under computation and the results will be published elsewhere.

Finally, we must remark that in favour of the self-organization in non-crystalline chalcogenides speaks the polymorphous-crystalloid model for the glasses developed by Minaev [38], and last but not least the paracrystalline model applied to chalcogenides by Popescu and Bradaczek [43].
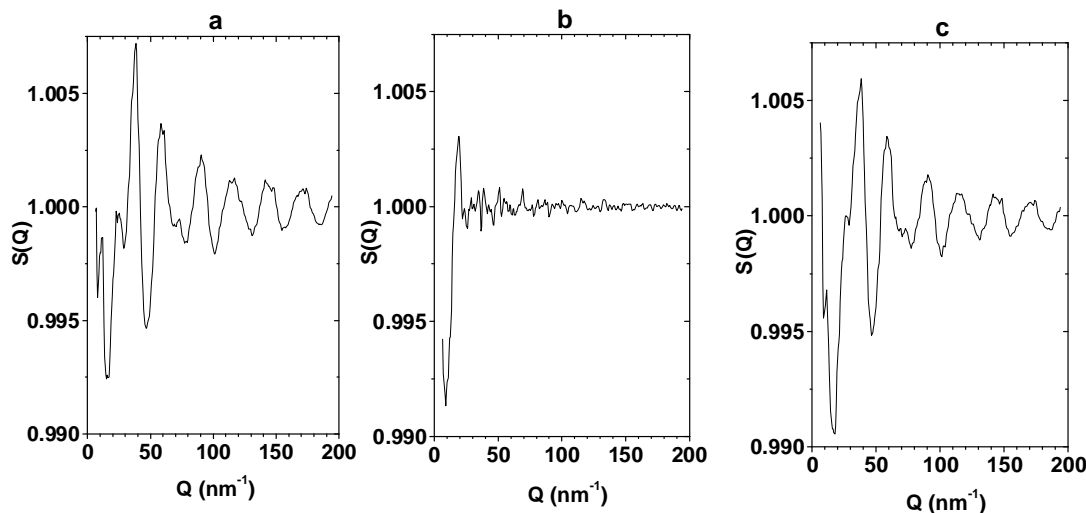

Fig. 2. The structure factor of the model with 802 atoms for As_2S_3; a. structure factor for the network of 802 atoms; b. structure factor for the void system; c. structure factor for the model with voids occupied by atoms.

4. Conclusions

The modelling of atomic scale structure of amorphous silicon and chalcogenide glasses have shown that nano-structuration in non-crystalline networks is a natural process occurring during network formation and is essentially a splitting of the continuous random network in nanometrically homogeneous domains. The inter-domain boundaries can be more or less ordered so that rms deviation of the bond-bending angle takes a minimum value. The nano-structuration of the non-

crystalline networks can be viewed as a new phenomenon in network glasses, which can be exploited for producing materials with controlled properties, useful in three-dimensional optoelectronic devices.

Acknowledgements

References

[1] I. Balberg, J. Optoelectron. Adv. Mater. **3**(3), 587 (2001).
[2] S. R. Ovshinsky, J. Non-Cryst. Solids, **32**, 17, 1979; S. R. Ovshinsky, Rosa Young, W.Czubatyj, Xuming Deng, U.S. Patent No. 5,103,284, April 7, 1992.
[3] D. L. Staebler, C. R. Wronski, Appl. Phys. Lett., **31**, 292, 1977.
[4] R. A. Street, J. Kakalios, C. C. Tsai, T. M. Hayes, Phys. Rev. B **35**, 1316, 1987.
[5] D. V. Tsu, Ben Chao, S. R. Ovshinsky, S. Guha, J. Yang, Appl. Phys. Lett. **71**, 1317, 1997.
[6] D. V. Tsu, S. Chao, S. R. Ovshinsky, S. J. Jones, J. Yang, S. Guha, R. Tsu, Phys. Rev. B **63**(12), 125338, 2001.
[7] D. E. Polk, J. Non-Cryst. Solids **5**, 365 (1971).
[8] P. Steinhardt, R. Alben, R. Weaire, J. Non-Cryst. Solids **15**, 199 (1974).
[9] M. Popescu, Ph. D. Thesis, Bucharest 1975.
[10] P. N. Keating, Phys. Rev. **145**(2), 637 (1966).
[11] R. M. Martin, Phys. Rev. B **1**(10), 4005 (1970).
[12] F. W. Lytle, D. E. Sayers, A. K. Eikum, J. Non-Cryst. Solids **13**, 69, 1973-1974.
[13] J. F. Graczyk, S. C. Moss, Proc. Intern. Conf. on the Physics of Semiconductors, Cambridghe Mass. 1970 (USAEC 1970), p. 658.
[14] R. Grigorovici, R. Manaila, Thin Solid Films **1**, 343 (1968).
[15] M. Popescu, J. Non-Cryst. Solids **192&193**, 140-144 (1995).
[16] R. Grigorovici, P. Gartner, I. Corcotoi, J. Non-Cryst. Solids, **114**, 256-258 (1989).
[17] J. Weissmüller, Nanostructured Materials **4**, 261 (1993).
[18]. S. R. Elliott, Nature **354**, 445 (1991).
[19]. K. O. Jensen, P. S. Salmon, I. T. Penfold, P. G. Coleman, J. Non-Cryst. Solids **170**, 57 (1994).
[20]. R. Grigorovici, J. Non-Cryst. Solids **35&36**, 1167 (1980).
[21]. I. Kaban, Th. Halm, W. Hoyer, J. Non-Cryst. Solids **288**, 96 (2001).
[22]. P. H. Gaskell, J. Non-Cryst. Solids **293-295**, 146 (2001).
[23]. Th. Halm, J. Nomssi Nzali, W. Hoyer, R. P. My, M. Bionducci, J. Non-Cryst. Solids **293-295**, 182 (2001).
[24] M. Popescu, J. Non-Cryst. Solids **35&36**, 549 (1980).
[25] F. Sava, J. Optoelectron. Adv. Mater. **5**(5),   2003).
[26] M. Popescu, J. Non-Cryst. Solids **75**, 477 (1985).
[27] J. P. DeNeufville, H. K. Rockstadt, in: Amorphous and Liquid Semiconductors, Eds. J. Stuke and W. Brenig, Taylor and Francis Ltd, London 1974, pp. 419.
[28] J. C. Phillips, J. Non-Cryst. Solids **34**, 153 (1979).
[29] M. F. Thorpe, J. Non-Cryst. Solids **57**, 355 (1983).
[30] P. Boolchand, D. G. Georgiev, B. Goodman, J. Optoelectron. Adv. Mater. **3**, 703 (2001),
[31] P. Boolchand, D.G. Georgiev, M. Micoulaut, J. Optoelectron. Adv. Mater. **4**, 823 (2002).
[32] D. G. Georgiev, P. Boolchand, M. Micoulaut, Phys. Rev. B, **62**, R 9228 (2000).
[33] Y. Wang, P. Boolchand, M. Micoulaut, Europhys. Lett. **52**, 633 (2000).
[34] P. Boolchand, W. Bresser, Nature **410**, 1070 (2001).
[35] D. G. Georgiev, P. Boolchand, H. Eckert, M. Micoulaut, K. Jackson, Europhys. Lett. **62**(1), 49 (2003).

[36] Y. Wang, T. Nakaokay, K. Murase, J. Optoelectron. Adv. Mater. **3**(3), 721 (2001).

[37] P. Boolchand, D. G. Georgiev, Tao Qu, Fei Wang, Liuchun Cai, Swapnajit Chakravarty,
     C. R. de l'Académie des Sciences (Paris), Chimie **5**, 713 (2003).

[38] V. S. Minaev, J. Optoelectron. Adv. Mater. **3**(2), 233 (2001).

[39] V. S. Minaev, J. Optoelectron. Adv. Mater. **4**(4), 843 (2002).

[40] M. Popescu, W. Hoyer, J. Optoelectron. Adv. Mater. **4**(4), 867 (2002).

[41] V. Lyubin, M. Klebanov, J. Optoelectron. Adv. Mater. **3**(2), 265 (2001).

[42] M. Popescu, J. Optoelectron. Adv. Mater. **3**(2), 279 (2001).

[43] M. Popescu, H. Bradaczek, J. Optoelectron. Adv. Mater. **3**(2), 249 (2001).